Conduction, Storage and Leakage in Particle-on-SAM Nano-Capacitors

Michael B. Cortie, Hadi Zareie, S. Ramesh Ekanayake, and Michael Ford

***Abstract*— Individual gold nanoparticles exhibit discrete capacitances of the order of 1 aF, and they can be tethered to a conductive substrate using a bi-functional monolayer of a suitable organic molecule. However the conduction, retention and leakage of charge by such an attached 'nano-capacitor' will be an important issue in any practical application of this concept. Here we investigate the electrical properties of the particles using a combination of scanning tunneling spectroscopy and numerical modeling based on equalizing WKB-style tunneling currents. Application of the model provides the voltage division across the structure, and together with an estimate of the capacitance of the particle, provides an indication of likely stored charge and energy, and its decay. The methodology was tested with I-V data measured for an Au{111}-α,α'-p-xylyldithiol-Au nanoparticle system in air. About 25 eV can be stored on the nanoparticles using a charging voltage of 3V, corresponding to up to twenty electrons. However, leakage of the charge will occur by tunneling in approximately $6x10^{-9}$ seconds. Therefore these nanocapacitors would discharge completely in any electric circuit slower than about 1.5 GHz.**

***Index Terms*—capacitance, dielectric films, leakage currents, nanotechnology**

I. Introduction

A number of nanoscale electronic devices have been proposed and investigated, amongst which 'molecular switches', diodes and the single electron transistor appear to be prominent [1]. Notwithstanding some setbacks occasioned by the Schön affair (in which false claims for functionality were made [2]), it seems that sentiment is generally still positive, and it is believed that useful functionality may be achieved from such nanoscale molecular devices [3]. Many of these putative nanoscale electronic circuits will require the incorporation of controlled quantities of capacitance. Of course the interconnects of such circuits will exhibit a degree of capacitance of their own, and charge may also be stored on transistors, but we believe that there may be a need at times for discrete capacitors. Although the thickness of the gate oxide layers of many existing commercial devices can already be as thin as two or three nm, we define 'nano-capacitors' here to be discrete capacitors in which the lateral (*x* and *y*) dimensions of the device are also in the nanoscale. Such devices do not exist yet in a commercial sense but have been proposed [4,5].

Nanoscale, single electron, parallel plate capacitors fabricated in a top-down fashion using electron lithography can be envisaged and could store about 0.4 eV per electron [4]. However the maximum potential difference possible across the plates will be limited by the breakdown of the dielectric between them at some sufficiently high value of electric field, E_{db}, and by current leakage due to electron tunnelling. The published bulk values of E_{db} for ceramic materials are in the range 0.01 to 0.2 MV/cm [6] , while that of air itself is only about 0.03 MV/cm. Clearly, not even existing ICs operating at say 2 V over a gate oxide thickness of 2 nm (a field of 10 MV/cm) could operate if the bulk values applied at the nanoscale. However, the so-called 'thickness effect' causes the E_{db} of dielectrics to increase as thickness decreases [4,7-10], which is the explanation for the use of these materials as nanoscale gate oxides, with dielectric strengths of around 9 to 15 MV/cm representing the current best-practice for nanoscale layers of oxides such as SiO_2 or Al_2O_3 respectively [11-14]. Current leakage becomes serious at field strengths > 6.5MV/cm, which will cause leakage currents of up to $1000A/cm^2$ [11,15,16].

Self-assembled nanocapacitors could be a possible alternative to a very small parallel plate capacitors. They will also have very high electric fields and quantized charge, and will be effected by the electron wavelength [17,18], ambient electromagnetic and thermal conditions, and oxidation. However, their possible advantage is that they would be compatible with the 'soft' electronics paradigm, in which the individual components are brought into position by the processes of 'self-assembly' from a liquid host medium. It is logical to use gold for the metallic portion of this and other nanoscale devices, following naturally from its unique resistance to oxidation and its useful thiophilic surface chemistry [19], while the dielectric layer of the device would logically be comprised of a mono- or bi-layer of oriented organic molecules [20]. Here we explore the performance of such capacitors using the well-known Au{111}-α,α'-p-xylyldithiol-Au system [20] as a prototype. Phenomena at ambient temperature and under atmospheric conditions were investigated since this was judged to be the likely operating environment of future molecular electronics devices.

Manuscript received September 8, 2004. M.B Cortie (phone: +61-2-9514-2208; fax: +61-2-9514-7553; e-mail: michael.cortie@ uts.edu.au), M.H. Zareie (hadi.zareie@ uts.edu.au), R. Ekanayake (srekanay@ uts.edu.au) and M. Ford (mike.ford@ uts.edu.au) are with the Institute for Nanoscale Technology, University of Technology Sydney, PO Box 123, Sydney NSW 2007, Australia.).

II. EXPERIMENTAL

A. Nanocapacitor geometry and characterisation

Systems of gold nanoparticles attached to self-assembled monolayers (SAMs) have been well-studied from a fundamental perspective [21-26]. An individual component is shown schematically in Fig.1, but in general there are many millions of such units assembled in parallel on a conductive substrate, usually also of gold. Charging of the capacitor can be demonstrated by bringing the tip of a scanning tunnelling microscope up to a particle, and applying a bias voltage $V_{bias}=V_{sub}-V_{tip}$, Fig. 1.

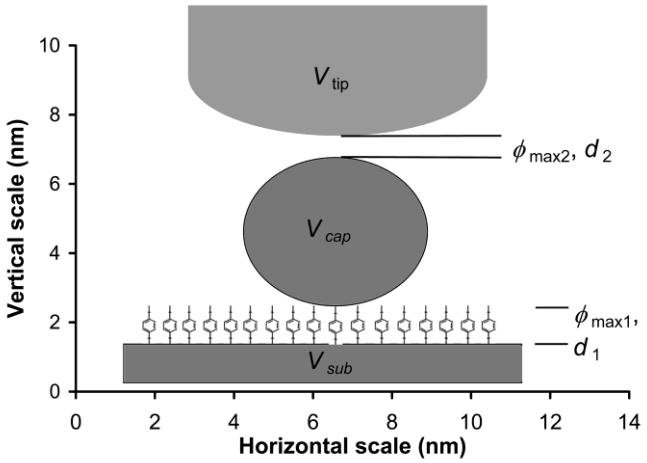

Fig. 1. Schematic diagram of the system studied, showing self-assembled monolayer of XYL (α,α'-p-xylyldithiol) molecules, gold nanoparticle and STM tip used for charging and characterization.

The capacitance of gold nanoparticles in electrolytes is known. As an example of the order of magnitudes involved, Chen *et al.* [27] obtained values of $5x10^{-19}$ to $1x10^{-18}$ F for particles of 2.2 nm diameter, corresponding respectively to particles capped with butanethiolate and 2-phenylethyl-thiolate, Li and Li [28] reported $1.13x10^{-18}$ F for 3.2 nm diameter particles capped with 3-mercapto-1,2-propanediol, Chaki *et al.* $1.6x10^{-18}$F for 3.7 nm particles capped with dodecanethiol [29], and Toyota *et al.* up to $2.5x10^{-16}$ for citrate-stabilized 11 nm diameter particles [30]. The macroscopic double layer capacitance of gold surfaces in an electrolyte is of the order of 7 to 20, and 60 to 160 μF/cm^2, for thiol-coated and naked surfaces respectively, with the variations being due in part to capacitance also being a function of the voltage at which it is determined and of the composition of the electrolyte [30,31]. The reported capacitances of the individual nanoparticles in an electrolyte are therefore consistent with a consideration of their surface area and double layer capacitance [30]. Quantised charging of such particles has been reported [27-29], and this evidently corresponds to the insertion or removal of charged ions at the particle surface. However, a gold particle can also be considered to have a self-capacitance that is independent of electrochemical capacitance, and the value of this depends on the radius of the nanoparticle, the thickness of the dielectric layer and its dielectric constant [27,28]

$$C = 4\pi\varepsilon_0\kappa\left(\frac{r}{d}\right)(r+d) \quad (1)$$

(1)

where κ is the dielectric constant of the SAM molecule or other moiety coating the particle, r the radius of the nanoparticle and d the thickness of the dielectric coating on the particle. Assuming a κ for XYL of 1.5 [20] and an r in our case of ~2.5 nm, then a C for the particle of $1.5x10^{-18}$ F is indicated. Alternatively, the capacitance of a bare, isolated sphere is given by

$$C = 4\pi\varepsilon_0 r \quad (2)$$

which would be $2.8x10^{-19}$ F in the present instance. Finally, the capacitance of a parallel plate capacitor of radius 2.5 nm and separation of 1.0 nm would be $3.6x10^{-19}$ F. We consider that these estimates straddle the true capacitance and will use an estimate of $1x10^{-18}$ F in the work to follow. In these expressions there is the further possibility of a small (~10%) correction to account for the Thomas-Fermi screening length of an electron [17,18], which we have however ignored.

As in most proposed nanoscale electronic devices, there is a problem of how to connect them into an electric circuit. In any case, the attraction of supposed molecular electronics circuitry is that interconnects would be molecular in nature too, so that the need for metallic wires would be dispensed with. However, here we, like many others, have invoked the use of an STM tip to pass current through the system, even though some other tunnelling geometry might be required in a real device.

The dielectric molecule chosen was α,α'-p-xylyldithiol (Fig. 2). This molecule, sometimes known as XYL, was selected because SAMs of it have been well studied [20,22,23], and because it is commercially available. The SAM was produced by steeping clean gold {111} surfaces in a 0.5 mM solution of XYL in methylene chloride for 24 hours. Gold nanoparticles were subsequently introduced onto the surface by dipping the SAM-coated samples for 24 hours in a colloidal suspension of 5 nm diameter citrate-stabilized gold nanoparticles purchased from Sigma. STM and STS measurements were performed on a Nanoscope III system operated in air at room temperature. Freshly-cut Pt-Ir tips (0.2 mm) were used. STM images and STS curves were obtained with typical tip-sample bias voltages of up to ±3V and tunneling currents up to 10 nA.

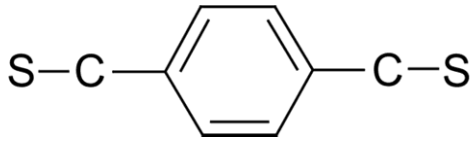

Fig. 2. The structure of the α,α'-p-xylyldithiol ('XYL') molecule used to produce the self-assembled monolayer.

B. Modelling of tunnelling and discharge currents

Although the I-V characteristic of a SAM-Au junction may be readily measured in a STM, the resulting data is the

convolution of two tunnelling currents, from V_{tip} to V_{cap}, and from V_{cap} to V_{sub}. However, both storage and leakage on the particle is determined by V_{cap}, which cannot be directly measured. Therefore, an analytical framework with which to model the system was required.

There is a rich literature devoted to the study of the tunnelling currents across tunnel junctions and to current conduction through so-called molecular wires [*e.g.* 32,33]. In general, while the currents may be in principle computed *ab initio*, this requires an accurate determination of diverse parameters. The calculated current is extremely sensitive to many of these input parameters [32] rendering a genuine *ab initio* approach problematic [33] since the computed results may be in error by one or two orders of magnitude [34, 35]. Therefore, in some cases a semi-empirical approach has been adopted [*e.g.* 22,36,37] and a model for tunnelling current is constructed by fitting experimental data to a chosen model. In our case we have simulated the nano-capacitor system as two tunnelling barriers in series. Barrier 1, V_{cap}-V_{sub}, is the 'dielectric barrier' and barrier 2, V_{tip}-V_{cap}, the 'air barrier'. Electrons tunnel through this circuit, and at any time an excess charge of Z electrons may be stored on the nanoparticle.

The tunnel barrier may be conceptually modelled using a trapezoid, the shape of which is defined by the parameters V_{sub}, V_{tip}, d (the width of the barrier) and ϕ_{max} (the height of the barrier without applied bias). However, this approach invokes a somewhat unrealistic shape of energy barrier since real barriers are rather more rounded due to the phenomenon of image charging. Nevertheless, the attraction of a trapezoidal barrier is that it is described by only four parameters, all of which are in principle readily determined. However, an alternative barrier profile that is more realistic in shape than the trapezoidal, but which is nevertheless also simply described, is possible; and it is based on an exponentiated segment of the sine function

$$\phi(z) = V_{sub}\left(1-\frac{z}{a}\right)+\phi_{\max}.\left[\sin\left(\frac{\pi.z}{a}\right)\right]^{m} \qquad (3)$$

provided V_{tip}=0.

This type of barrier takes up the effect of image charges in an empirical way and bundles them into an effective value for the ϕ_{max}. The strategy of folding diverse barrier parameters into an 'effective' barrier height is not new [16,36,37] but we believe (4) is a novel and useful form. The shape of the barrier in (4) is controlled by the geometric parameter m. In the limit as $m\rightarrow 0$, the barrier becomes trapezoidal (Fig. 3) and there are no effects due to image charging. If m is set to 0.2 then a barrier with a shape similar to those reported in the prior literature with image charging is obtained. The barriers are compared in Fig. 3, for a bias voltage of 1 volt, a tunnel distance of 2 nm, and a barrier height of 2 eV. The potential of the tip is taken as ground, at 0 eV. So-called 'band bending' is ignored in this approach with any influence of it being taken up in the empirical fit of the barrier profile.

The expressions for $\phi(z)$ may be used to generate an expression for tunnelling probability based on the WKB approximation [38] :

$$T(E) = e^{-\frac{2\sqrt{2}}{\hbar}\int_0^d \sqrt{m((\phi(z)-E)}dz} \qquad (4)$$

where E the energy of the incident electron and m is its mass.

We have performed the integration numerically, using the trapezoidal rule and a step size of d/100. Data for $T(E)$ using this model are shown in Fig. 4 for a tunnelling distance of 1 nm and a barrier height of 1 eV. In each case the curves for $T(E)$ are terminated at the top of the substrate's electron distribution, since we have assumed a sharp cut-off at the Fermi level. These curves represent a substantial simplification over those predicted from a more rigorous analysis of the electronic structure of the molecule and substrates [*e.g.* 20,32,33] but we will show that they are adequate for the present purpose.

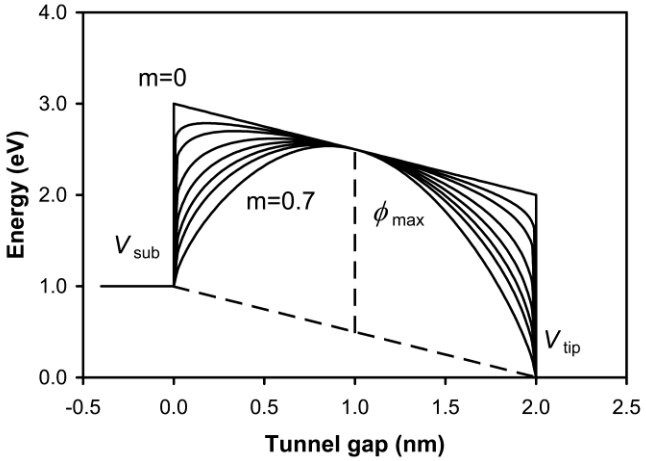

Fig. 3. Energy band diagram showing the effect of parameter m on shape of barrier defined by V_{sub}, V_{tip}, d and ϕ_{max}.

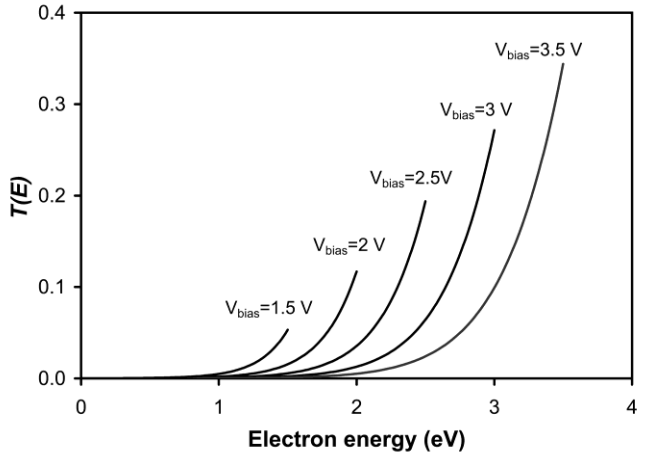

Fig. 4. Curves of transmission probability $T(E)$ calculate for a barrier gap of 1 nm and a barrier height of 1 eV using the exponentiated sinusoidal barrier defined in (4) and m=0.2.

When V_{bias} >> kT (which is ~0.03eV at room temperature), and assuming a constant and equal density of states fully occupied up to identical Fermi levels in both substrate and tip [*e.g.* 39], and the usual conventions that set V_{tip}= ground= 0 V and regions of more negative electric potential to more positive values of E, then the net difference between the forward and reverse tunnelling currents across the barrier is given by

$$i = A' \int_0^{V_{sub}} \rho_{sub}(E+V_{bias}).\rho_{tip}(E)T(E)dE \qquad (5)$$

where $\rho_{sub}(E+V_{bias})$ is the density of states of the substrate after application of the bias voltage, and A' is a geometric parameter that takes into account the number of electrons available for tunnelling as a result of variations in cross-sectional area and bulk electron density, and the dimensional requirements of (6). In this scheme no tunnelling of electrons with E<0 occurs because there is nowhere for them to go in the band structure of the tip since it is fully occupied, while there is no need to integrate beyond V_{sub} because the substrate has no electrons for which E>V_{sub}. We note that an assumption of constant density of states in the substrate is reportedly close to the actual situation [39], however the DOS of the tip and nanoparticle will be more complex in reality, a factor which would introduce an polarity-induced asymmetry into the tunnelling currents [39].

It is appreciated that further complexity would be introduced into the band structure of the gold substrate, the gold nanoparticle and the microscope tip when V_{bias} is applied. However, for the purpose of the present exercise we allow

$$P_{sub}(E)=B \text{ for } E \le V_{sub}, \text{ and } P_{sub}(E)=0 \text{ for } E>V_{sub} \qquad (6)$$

where $P(E)$ is the actual occupancy of the states defined by $\rho(E)$, and B is a constant. So the expression for tunnelling current becomes

$$i = A\int_{V_i}^{V_j} T(E)]dE \qquad (7)$$

where $A = A'.B$ and $V_j \le V_{sub}$.

Under equilibrium conditions $i_1=i_2$, therefore allowing the two tunnelling currents to be equated. If no charge is stored on the nanoparticle, then we could, as a first approximation, have used a linear division of voltage to obtain V_{cap}. However, since the particles have capacitance, the possibility of retained charge on them must be considered. The effect of the stored charge is to raise or lower the potential of the particle from that predicted from a linearly-derived electrostatic potential.

The profile of the composite tunnelling barrier is shown in Fig. 5. In accordance with convention, a positive bias on an STS curve corresponds to tunnelling current from STM tip to substrate [39], which however occurs by *electrons* flowing from substrate to tip. However, the numerical expressions invoked here are symmetrical with respect to the direction of electron flow.

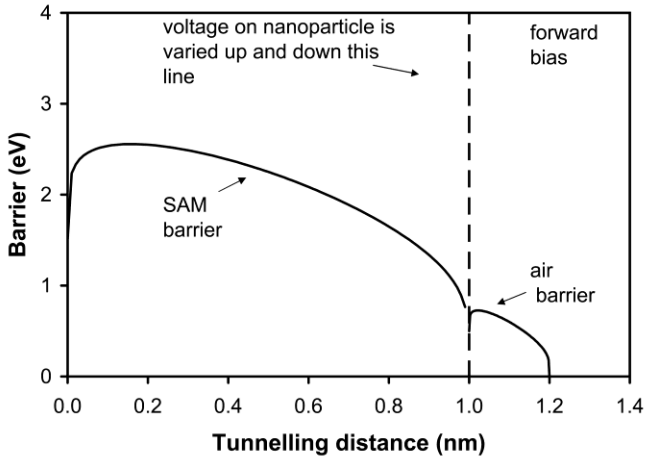

Fig. 5. Energy band diagram for nanocapacitor for conditions of 2.0 V forward bias. The voltage of the nanoparticle is iteratively varied along the indicated line to equalize the two tunnelling currents.

A program to repetitively evaluate and fit an I-V curve using (7) was written in Delphi Pascal™ and checked for numerical accuracy using Mathematica™. In this the value of V_{cap} was systematically varied to make $i_1 = i_2$ to within 1% for each value of V_{bias}. The result of each iteration was a computed composite I-V curve that depended upon the values chosen for ϕ_{max1}, ϕ_{max2}, d_1, d_2, A_1 and A_2. In the present work we have captured the effect of possible asymmetries in current flow with polarity in our model by allowing the ϕ_{max} parameters to be split, if necessary, into a forward ϕ_{maxfwd} and a reverse, ϕ_{maxrvs} parameter. The routine to balance the tunnelling currents was placed inside a loop that randomly generated new values of parameters selected for optimization, and the process repeated in a Monte Carlo fashion to drive down the square of the errors of the fit. Both the step size and the directions of change chosen were random.

However, in its basic form this model has too many unknowns for reliable application to a single I-V curve. The problem can be simplified by noting that the thickness of an XYL monolayer is known to be 0.83 nm [22] to which should be added the length of the Au-S bond (~0.2 nm) to yield an effective d_1 of 1.0 nm [23]. In the case of barrier 2, the minimum possible d_2 for stable STM operation is known to be of the order of 0.15 nm for the imaging and STS conditions used here, while ϕ_{max2}, the barrier height between STM tip and gold has been reliably reported to be in the range 0.31 to 0.97 eV, depending on method of preparation of the gold [40,41]. This is much less than the value of ~4.5 eV for gold in vacuum, which in turn is somewhat less than the work function of Au (5.1eV) due to the effects of image charging. The low barrier height for gold in air is believed to be due to the effects of adsorbed contaminants [40,42]. However, the situation is complex and it has been shown that ϕ_{max} can be as high as 11.3 eV in humid air if extremely large electric fields (~200 MV/cm) are present [36]. Fortunately, an analysis of the present double tunnelling model showed that, provided d_2 is small, the system was not particularly sensitive to the value of ϕ_{max2} used, even over the range of uncertainty cited. Nevertheless we have made our own determination of ϕ_{max2}

during the course of obtaining A_2. The method by which these two parameters was established will now be described.

STS data were measured on a bare Au{111} surface in air for three different set points, A, B and C, corresponding to three unknown values of d_2. Application of the model to each data set produced a continuum of different A_2 , ϕ_{max2}, and d_2 values of equally credible coefficient of correlation, and it was not possible to determine the correct ones from analysis of a single data set. However, the trends of the three sets of data converge, Figure 6, and a common value of A_2 of ~2.0×10^{21} nA was indicated. Further refinement of the optimization indicated that ϕ_{max2} was in the range 0.35±0.21 eV and that the best-fitting d_2's for the three data sets were 0.15, 0.28 and 0.35 nm, Fig. 7. The value of ϕ_{max2} is within the range reported by Boyer [40] but was obtained here without any prior assumptions. The values of d_2 are also credible. The results of fitting the model with further relaxation of ϕ_{max2} into $\phi_{max2fwd}$ and $\phi_{max2rvs}$, are shown in Fig. 8.

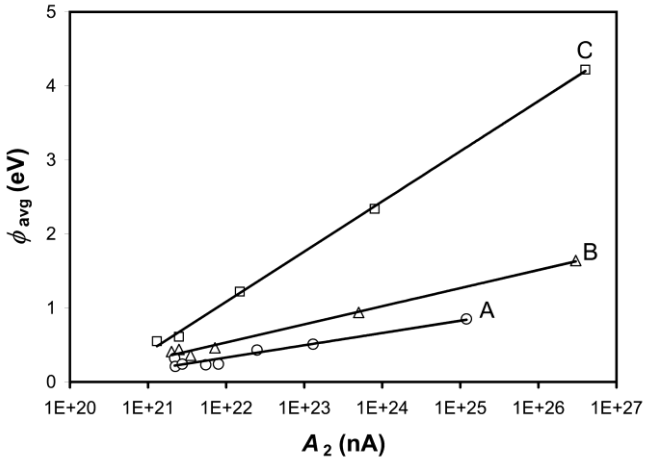

Fig. 6. The best-fitting values of A_2 and ϕ_{max2} for each of the three experimental data sets are plotted. The trends converge on values of about 2×10^{21} nA and 0.35 eV.

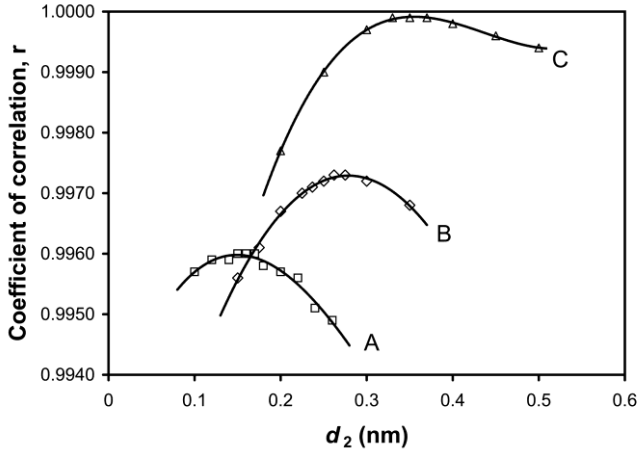

Fig. 7. Determination of the STM tip-substrate distances, d_2 for the three data sets. The most probable value of d_2 in each case is that corresponding to the maximum of each curve.

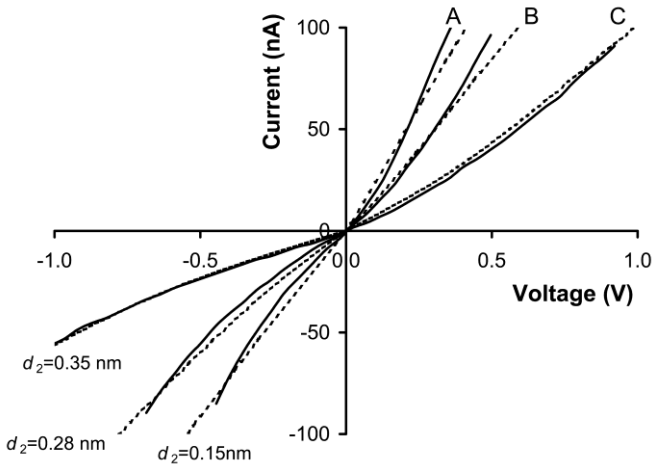

Fig. 8. Scanning tunnelling spectra measured on a naked Au {111} surface using the standard tip, with set of calculated tunnelling curves superimposed.

III. Results

A. Microstructure

An image of the upper surface of the SAM prior to the application of the gold nanoparticles is shown in Fig. 9. The XYL molecules are in an upright orientation and the size of the individual defect-free domains of the order of 5 nm. An image of the surface after the addition of the top layer of gold nanoparticles is shown in Fig. 10. It is evident that the gold nanoparticles are sparsely distributed over the surface, with interparticle distances being of the order of 20 nm.

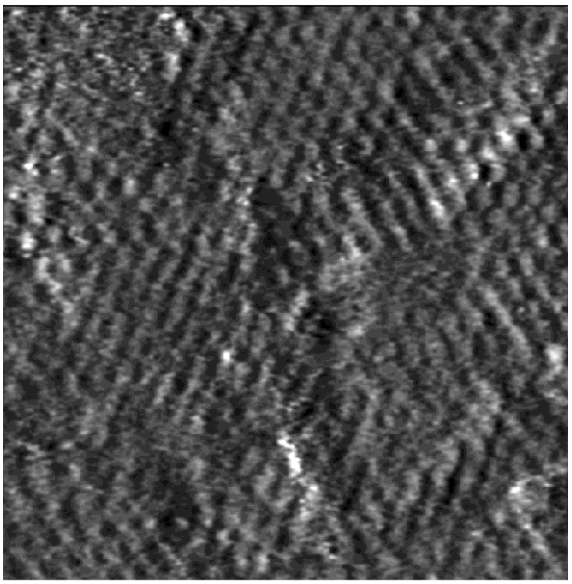

Fig. 9. Image of the top layer of the XYL SAM showing individual, upright, molecules, image is 15x15 nm.

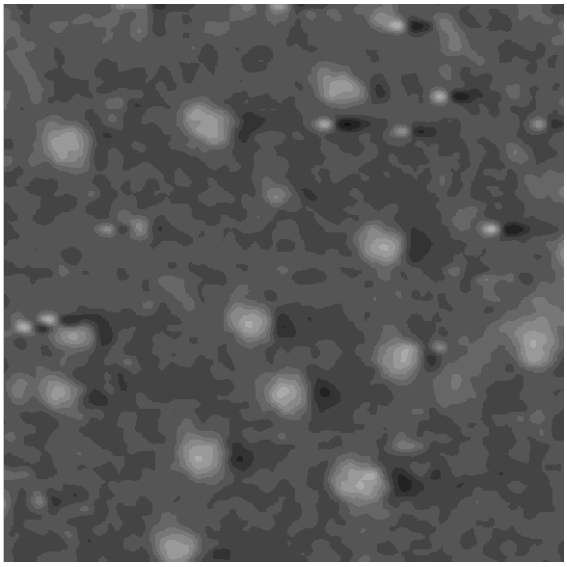

Fig. 10. Image of the completed nanocapacitor system showing gold nanoparticles attached on the top of the XYL SAM, image is 100x100 nm.

B. Measured and calculated tunnelling currents

A series of STS scans of the same particle but with different stand-off distances (d_2) was performed to isolate the ϕ_{max1} and A_1 parameters, as described previously for the bare Au surface. However, even though d_2 was varied in this series of calculations from 0.15 to 0.85 nm, the optimum A_1 only varied from 1.93×10^{22} nA to 2.64×10^{22} nA and the associated values of ϕ_{max1} only varied from 0.77 to 0.81 eV, Fig. 11. It is obvious that the value of d_2 has only a small influence on the outcome. The reason for this is that the STM tip was intentionally placed close to the gold nanoparticle, and the tunnelling current of the composite system was dominated by the resistance offered by the SAM. The best-fitting values of ϕ_{max1} are indicated in Fig. 12 for data taken off this particle. I-V curves produced with less than the optimum value of ϕ_{max1} were too straight with dI/dV at V=0 being too high, whereas those produced with greater than the optimum value of ϕ_{max1} were increasingly inflexed, with a low value of dI/dV at V=0. The average value of the optimum $\phi_{max1fwd}$ and $\phi_{max1rvs}$ for the five data sets was 0.76 eV (s=0.12 eV) and 0.77 eV (s=0.07 eV) respectively and that of A_1 was 1.80×10^{20} nA (s=0.36×10^{20} nA). In these and other calculations in this section ϕ_{max2} , A_2 and m were fixed at 0.35 eV, 2.0×10^{21} nA and 0.2 respectively.

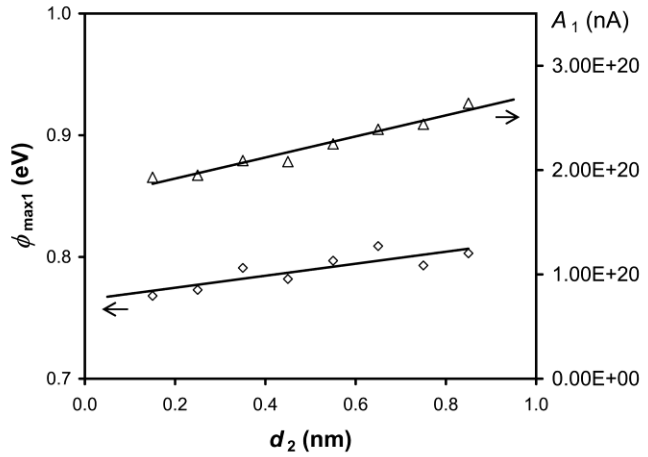

Fig. 11. Effect of different assumed values of d_2 on the best-fitting values of A_1 and ϕ_{max1} for the experimental data from the Au-SAM-Au system.

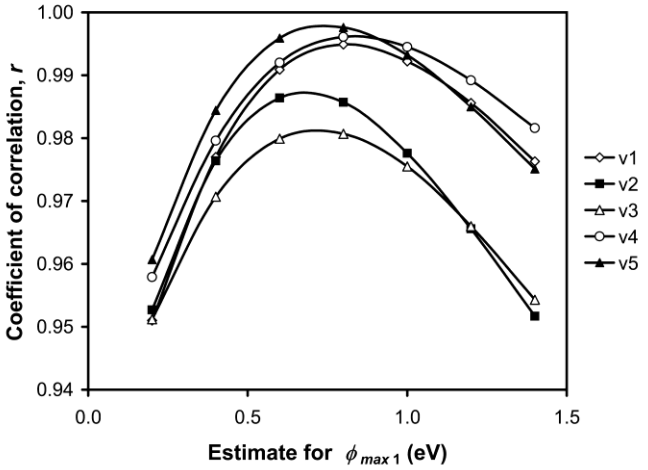

Fig. 12. Coefficients of correlation plotted for different assumed values of ϕ_{max1}, for different scans of the same particle, showing that the nominal value of this parameter lies in the vicinity of 0.75 eV.

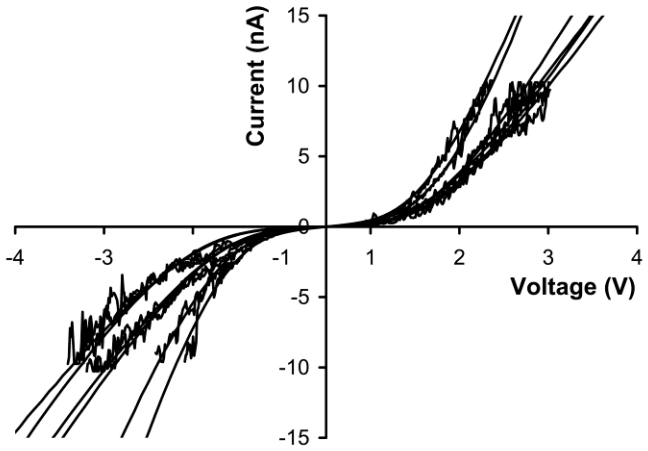

Fig. 13. Examples of tunnelling spectra taken through gold nanoparticles on XYL SAM with superimposed calculated spectra.

TABLE 1. PARAMETERS OBTAINED FOR THE TUNNELING CURRENT MODEL.

Sample	ϕ_{max1}, eV		d_2, nm	A_1, nA	Coeff. of
	forward	reverse			correlation, r
192	0.70	0.87	0.25	$6.07\text{x}10^{20}$	0.9911
194	0.65	0.80	0.23	$4.62\text{x}10^{20}$	0.9960
195	0.69	0.68	0.25	$4.68\text{x}10^{20}$	0.9945
196	0.71	0.70	0.26	$5.30\text{x}10^{20}$	0.9975
Pt3	0.78	0.72	0.21	$1.30\text{x}10^{21}$	0.9973
Pt4	0.69	0.73	0.23	$9.87\text{x}10^{20}$	0.9983
average	0.70	0.75	0.24	$7.26\text{x}10^{20}$	-

The superimposition of the model onto spectra measured for six other nanoparticles is shown in Fig. 13 and Table I. Optimization was started at A_1=1.8x10^{20} nA, ϕ_{max1}=0.76 eV and d_2=0.25 nm, with variables being relaxed in that order. In general the curves are slightly asymmetric, but there appears to be no statistically valid difference between the average barrier height for the forward bias condition (tip is positive with respect to substrate) compared to the reverse state, i.e. $\phi_{max1fwd} \approx \phi_{max1rvs}$. Furthermore, like ϕ_{max2}, ϕ_{max1} is not expected to vary between experiments so the small difference between the various curves is due mainly to small variations in A_1, which depends in part on particle cross-section, and d_2.

IV. DISCUSSION

A. Voltage and stored charge

The voltage drop V_{tip}-V_{cap} predicted by the model was small, as expected, and rose to 0.15 ± 0.06 V at an applied bias of ±3 V. If the STM tip could be instantaneously removed or isolated at a total applied bias of 3 V, then the voltage left on the nano-capacitor at that instant would be 2.85 V. The corresponding electrical energy calculated for sample '192' of Table I due to a self-capacitance of ~1x10^{-18} F and integer numbers of stored electrons is shown in Figure 14, as a function of maximum applied bias. A particle diameter of 5 nm has been assumed for these calculations. Up to 17 e^- can be stored at 3 V according to these assumptions, however in practice care would have to be taken to verify that the SAM was not damaged at such high bias. In particular, desorbtion of the SAM molecules would be a possibility.

B. Lack of evidence for a Coulomb blockade

The stored energy on the particle reaches 25 eV at ±3 V. Given that kT is only about 0.03eV at room temperature, the question might be raised of whether a Coulomb blockade occurred here during the charging process. Certainly some workers, e.g. [21] have interpreted a flattened portion of an I-V curve near the origin (see Fig. 13, -1 V to +1 V) to be the result of such a blockade. However, I-V curves with these characteristics result naturally from the application of our double junction tunnelling model, and are common in I-V curves of SAMs without gold nanoparticles, e.g. [15], in any case. Therefore care should taken before ascribing such a gap to the effects of a blockade. In any event, the voltage (e/C) and energy (e^2/2C) changes due to a single electron charge transfer to a capacitor of 1x10^{-18} F are 0.16 V and 0.08 eV respectively (see steps in Fig 14), values that could be readily masked in the present data. Therefore we conclude that there is no evidence for a Coulomb blockade here.

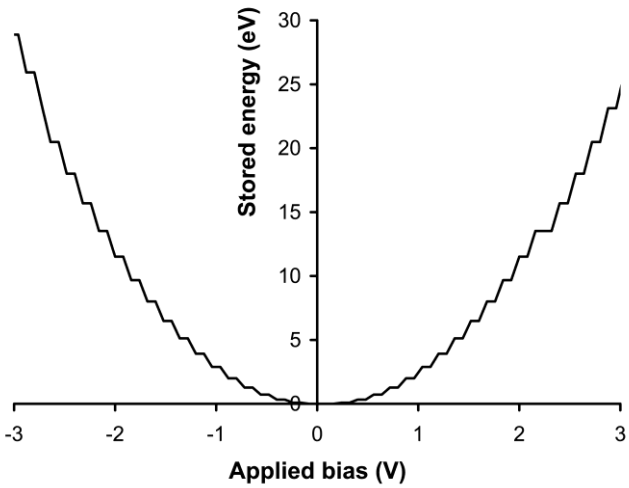

Fig. 14. Stored energy on nanocapacitor before onset of discharge using potential difference between particle and substrate calculated for sample '192', and a capacitance of 1x10^{-18} F.

C. Leakage of charge

Given that charge is placed on these 'nanocapacitors' by tunnelling, it follows that it will leak away by the same mechanism. Leakage currents in general have important practical implications, and much current research is focussed on maintaining capacitance while reducing leakage currents. The benchmark dielectric for microelectronics is SiO_2 and leakage currents through commercially applied SiO_2 barriers are in the range of 1 to 100 A/cm^2, depending on applied bias and barrier thickness [11,15,16]. However, it is believed [15] that a SAM can potentially offer matching or superior performance, especially compared to a SiO_2 barrier of only 1 nm thickness. Of course, the integration of a SAM into current designs of MOS or MIM capacitors is not possible, and a SAM is more likely to find application in some new generation, 'bottom-up' process for making devices.

The leakage current of the gold particles is given by (7) and Table I, with the tunnelling current between tip and particle set to zero. To achieve the latter the particle must somehow be electrically isolated once charged by physically withdrawing the tip. Thereafter the capacitor would discharge to the substrate. The discharge will be a stochastic process, and will proceed as single electron events. In the case of a particle of 1x10^{-18} F capacitance the leakage currents predicted by our model at voltages of 0.8, 1.6 and 3.2 V are 0.6, 3.7 and 16 nA respectively (assuming a ϕ_{max1} of 0.70 eV and A_1 of 4.7x10^{20} nA for the barrier). These correspond to tunnelling rates of ~4x10^9 , 2x10^{10} and 1x10^{11} electrons/per second. A simulation of the process is shown in Fig. 15, however tunnelling will be a stochastic process and the curve shown is idealistic. On average, a particle that is initially charged to 3.0 V will discharge to 0.5 V in about 2 ns, and will be completely discharged in 6 ns. If we assume a working range of 0.5 to 3.0

V and that the AC frequency of the host circuit should be at least three times faster than the time taken to discharge this amount, then we get a lower limit on usable circuit frequency of about 1.5 GHz.

At 1 volt bias the leakage currents are of the order of $6x10^3$ A/cm^2 (corresponding to 1.2 nA leaked over the mid-section of a particle of 5 nm diameter), and are of the same order as those reported for SAMs of dodecanethiol or for 1.0 nm SiO_2 under similar bias [15].

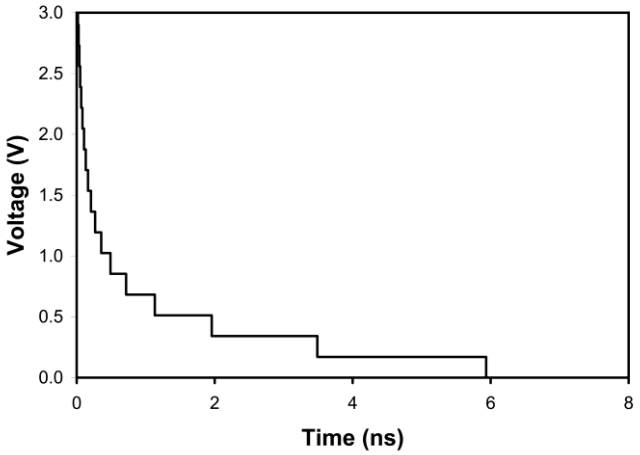

Fig. 15. Idealized discharge characteristic of the particle designated '192' in Table I, showing that voltage will decay to 0.5 V in 2 nanoseconds, and to 0 V in 6 ns, as a result of electrons tunneling into the substrate.

D. Barrier height in the SAM

The height of the energy barrier in the SAM (ϕ_{max1}) is one of the parameters required by the model, and controls the rate of discharge of the particle. We have shown here that it is ~0.75 eV for α,α'-p-xylyldithiol. This parameter might reasonably be expected to reflect the energy difference between the LUMO of α,α'-p-xylyldithiol and the Fermi levels of the bulk gold and gold nanoparticle. One can gain a crude alternate estimate of this quantity from the magnitude of the HOMO-LUMO gap of the isolated molecule and by assuming that the Fermi energy lies half-way between these orbitals. The HOMO-LUMO gap in this conjugated molecule has been calculated to be of the order of 4 eV, which is considerably less than the 6 to 8 eV expected for alkanes [20]. However, the molecule in the experimental system is not isolated from the electrodes and hybridisation will occur between the molecular orbitals and those of the bulk and the nanoparticle. This can have a strong effect on orbital energies relative to the Fermi level; for example, the absorption of CO onto a Ni surface causes hybridisation which drags the unoccupied 2π orbital of CO below the Fermi energy of the metal [35,43]. This phenomenon will considerably reduce the ostensible barrier height across a molecule. In support of this, measured values of ϕ_{max} for alkanethiols are in the range of only 1.1 to 3 eV [15,37], rather than the expected 3 to 4 eV.

REFERENCES

[1] S.M. Goodnick and J. Bird, "Quantum-effect and single-electron devices", *IEEE Transactions on Nanotechnology*, vol. 2, no. 4, pp.368-385, 2003.
[2] *New Scientist*, 5th October 2002, p.3.
[3] T. Choi and M. Stoneham, "Was Schön ever right?" *Materials Today*, vol. 7, no. 4, p.64, 2004.
[4] S.R. Ekanayake, M.B. Cortie, and M. Ford, "Design of deep-nanometer-scale capacitors and associated materials challenges", *Current Applied Physics* vol. 4, pp.250-254, 2004.
[5] G. Oldfield, T. Ung, and P. Mulvaney, "Au@SnO_2 core-shell nanocapacitors", *Advanced Materials*, vol. 12, no. 20, pp.1519-1522, 2000.
[6] *CRC Handbook of Chemistry and Physics*, 77th ed. Chemical Rubber Publishing Company, Cleveland, Ohio, 1997.
[7] J.J. O'Dwyer, *The Theory of Dielectric Breakdown of Solids*, Clarendon Press, Oxford, 1964.
[8] J.J. O'Dwyer, *The Theory of Electrical Conduction and Breakdown in Solid Dielectrics*, Clarendon Press, Oxford, 1973.
[9]J.M. Herbert, *Ceramic Dielectrics and Capacitors*, Gordon and Breach Science Publishers, New York, 1985.
[10] M.A. Alam, R.K. Smith, B.E. Weir, and P.J. Silverman, "Uncorrelated breakdown of integrated circuits", *Nature*, vol. 420, p. 378, 2002.
[11] L. Larcher, A. Paccagnella, and G. Ghidini, "Gate current in ultrathin MOS capacitors: a new model of tunnel current", *IEEE Transactions on Electron Devices*, vol. 48, pp.271-278, 2001.
[12] P. Ericsson, S. Bengtsson, and J. Skarp, "Properties of Al_2O_3 films deposited on silicon by atomic layer epitaxy", *Microelectronic Engineering*, vol. 36, pp.91-94, 1997.
[13] D.A. Buchanan, J.H. Stathis, E. Cartier, and D.J. DiMaria, "On the relationship between stress induced leakage currents and catastrophic breakdown in ultra-thin SiO_2-based dielectrics", *Microelectronic Engineering* vol. 36, pp.329-332, 1997.
[14] R. Aparicio and A. Hajimiri, "Capacity limits and matching properties of integrated capacitors", *IEEE J. Solid-State Circuits*, vol. 37, pp.384-393, 2002.
[15] A.P. Labonte, S.L. Tripp, R. Reifenberger, and A. Wei, "Scanning tunneling spectroscopy of insulating self-assembled monolayers on Au(111)", *J. Phys. Chem.*, vol. 106, pp.8721-8725, 2002.
[16] F. Jiménez-Molinos, F. Gámiz, A. Palma, P. Cartujo, and J.A. López-Villanueva, "Direct and trap-assisted elastic tunneling through ultrathin gate oxides", *J. of Applied Physics*, vol. 91, no. 8, pp.5116-5124, 2002.
[17] C.T. Black and J.J. Welser, "Electric-field penetration into metals: consequences for high-dielectric-constant capacitors", *IEEE Trans. on Electron Devices*, vol. 46, no. 4, pp.776-780, 1999.
[18] S.R. Ekanayake, B.S. Rodanski, M.B. Cortie, and M.J. Ford, "Quantum electrical characteristics of nanocapacitors", in *Proc. IEEE-Nano 2003*, The Institute of Electrical and Electronics Engineers, Piscataway, New Jersey, 2003, pp.756-759.
[19] M.B. Cortie, "The weird world of nanoscale gold", *Gold Bulletin*, vol. 37, pp.12-19, 2004.
[20] R.P. Andres, S. Datta, D.B. Janes, C.P. Kubiak, and R. Reifenberger, "The design, fabrication, and electronic properties of self-assembled molecular nanostructures", in *Handbook of Nanostructured Materials and Nanotechnology*, H.S. Nalwa Ed., Orlando : Academic Press, 2000, pp.179-231.
[21] T. Ohgi and D. Fujita, "Single electron charging effects in gold nanoclusters on alkanedithiol layers with different molecular lengths", *Surface Science* , vol. 532–535, pp. 294–299, 2003.
[22] R.P. Andres, T. Bein, M. Dorogi, S. Feng, J.I. Henderson, C.P. Kubiak, W. Mahoney, R.G. Osifchin, and R. Reifenberger, "Coulomb staircase at room temperature in a self-assembled molecular nanostructure", *Science*, vol. 272, pp.1323-1325, 1996.
[23] M. Dorogi, J. Gomez, R. Osifchin, R.P. Andres, and R. Reifenberger, "Room-temperature Coulomb-blockade from a self-assembled molecular nanostructure", *Physical Review B*, vol. 52, no.12, pp.9071-9077, 1995.
[24] D. Bethell, M. Brust, D.J. Schiffrin, and C. Kiely, "From monolayers to nanostructured materials : an organic chemist's view of self-assembly", *J. of Electroanalytical Chemistry*, vol. 409, pp.137-143, 1996.
[25] T. Ohgi, H.Y. Sheng, and H. Nejoh, "Au particle deposition onto self-assembled monolayers of thiol and dithiol molecules", *Applied Surface Science*, vol. 130-132, pp.919-924, 1998.

[26] N. K. Chaki, T. G. Gopakumar, T. Maddanimath, M. Aslam, and K. Vijayamohanana, "Effect of chain length on the tunneling conductance of gold quantum dots at room temperature", *J. of Applied Physics*, vol.94 no.5, pp.3663-3665, 2003.
[27] S. Chen, R.W. Murray, and S.W. Feldberg, "Quantized capacitance charging of monolayer-protected Au clusters", *J. Phys. Chem. B.*, vol. 102, pp.9898-9907, 1998.
[28] D. Li and J. Li, "Preparation, characterization and quantized capacitance of 3-mercapto-1,2-propanediol monolayer protected gold nanoparticles", *Chemical Physics Letters*, vol. 372, pp.668-673, 2003.
[29] N.K. Chaki, P. Singh, C.V. Dharmadhikari, and K.P. Vijayamohanan, "Single-electron charging features of larger, dodecanethiol-protected gold nanoclusters: electrochemical and scanning tunneling microscopy studies", *Langmuir*, in press, August 2004.
[30] A. Toyota, N. Nakashima, and T. Sagara, "UV–visible transmission–absorption spectral study of Au nanoparticles on a modified ITO electrode at constant potentials and under potential modulation", *Journal of Electroanalytical Chemistry*, vol. 565, pp.335-342, 2004.
[31] M. Petri, D. M. Kolb, U. Memmert, and H. Meyer, "Adsorption of mercaptopropionic acid onto Au(1 1 1). Part I. Adlayer formation, structure and electrochemistry", *Electrochimica Acta*, vol. 49, pp.175-182, 2003.
[32] L.E. Hall, J.R. Reimers, N.S. Hush, and K. Silverbrook, "Formalism, analytical model, and *a priori* Green's-function-based calculations of the current–voltage characteristics of molecular wires", *Journal of Chemical Physics*, vol. 112, no. 3, pp.1510-1521, 2000.
[33] A. Nitzan, and R.A. Ratner, "Electron transport in molecular wire junctions", *Science*, vol. 300, pp.1384-1389, 2003.
[34] S.T. Pantelides, M. Di Ventra, N.D. Lang, and S.N. Rashkeev, "Molecular Electronics by the Numbers", *IEEE Transactions on Nanotechnology*, vol. 1, no. 1, pp.86-90, 2002.
[35] K. Stokbro, J. Taylor, M. Brandbyge, J.L. Mozos, and P. Ordejón, "Theoretical study of the nonlinear conductance of di-thiol benzene coupled to Au(1 1 1) surfaces via thiol and thiolate bonds", *Computational Materials Science*, vol. 27 , pp.151-160, 2003.
[36] A.L. Korotkov, M. Bowman, H.J. McGuinness, and D. Davidovic, "Influence of H_2O molecules on sub-nanometre scale gaps between Au leads", *Nanotechnology*, vol. 14, pp.42-45, 2003.
[37] W. Wang, T. Lee and M. A. Reed, "Mechanism of electron conduction in self-assembled alkanethiol monolayer devices", *Physical Review B*, vol. 68, 035416, 2003.
[38] J. Singh, *Modern Physics for Engineers*, Wiley:New York, 1999.
[39] A.I. Onipko, K. Berggren, F. Yu, O. Klymenko, L.I. Malysheva, J.J.W. Rosink, L.J. Geerligs, E. van der Drift, and S. Radelaar, "Scanning tunneling spectroscopy on p-conjugated phenyl-based oligomers: A simple physical model", *Physical Review B*, vol. 61, no. 16, 11118-11124, 2000.
[40] L. Boyer, S. Noël, and F. Houzé, "Apparent tunnel barrier heights of PtIr–Au interfaces in relation to the Au surface composition", *J. Vac. Sci. Technol. B*, vol.16, no.4, pp.2006-2012, Jul/Aug 1998.
[41] M-B. Song, J-M. Jang, S-E Bae, and C-W. Lee, "Charge transfer through thin layers of water investigated by STM, AFM and QCM", *Langmuir*, vol.18, pp. 2780-2784, 2002.
[42] G. Seine, R. Coratger, A. Carladous, F. Ajustron, R. Pechou, and J. Beauvillain, "Tip-to-surface distance variations vs voltage in scanning tunneling microscopy", *Physical Review B*, vol.60 no.5, pp.11045-11050, October 1999.
[43] A. Zangwill, *Physics at Surfaces*, Cambridge University Press: Cambridge, 1988.